

## 키토산 피복/비피복 붕소 나노입자의 합성 및 분석, 그리고 항균효과 체외평가

Rukiye Sevinç Özakar<sup>#</sup>, Mehmet Semih Bingöl<sup>\*</sup>, Mehmet Cemal Adıgüzel<sup>\*\*</sup>, and Emrah Özakar<sup>#,†</sup> 

Department of Pharmaceutical Technology, Faculty of Pharmacy, Atatürk University

<sup>\*</sup>Eastern Anatolia High Technology Application and Research Center (DAYTAM), Atatürk University

<sup>\*\*</sup>Department of Microbiology, Faculty of Veterinary Medicine, Atatürk University

(2022년 6월 30일 접수, 2022년 9월 14일 수정, 2022년 9월 18일 채택)

## Preparation, Characterization of Chitosan-Coated/Uncoated Boron Nanoparticles and *In-Vitro* Evaluation of Their Antimicrobial Effects

Rukiye Sevinç Özakar<sup>#</sup>, Mehmet Semih Bingöl<sup>\*</sup>, Mehmet Cemal Adıgüzel<sup>\*\*</sup>, and Emrah Özakar<sup>#,†</sup> 

Department of Pharmaceutical Technology, Faculty of Pharmacy, Atatürk University, 25240 Erzurum, Türkiye

<sup>\*</sup>Eastern Anatolia High Technology Application and Research Center (DAYTAM), Atatürk University, 25240 Erzurum, Türkiye

<sup>\*\*</sup>Department of Microbiology, Faculty of Veterinary Medicine, Atatürk University, 25240 Erzurum, Türkiye

(Received June 30, 2022; Revised September 14, 2022; Accepted September 18, 2022)

**Abstract:** Many studies have reported that the widespread use and abuse of antibiotics have led to the emergence of multidrug-resistant bacteria, a significant weakness of current antibiotic therapy. Therefore, the present scenario motivates scientists to develop biocompatible nanoparticles (Nps) that apply better antibacterial effects and biocompatible properties, including cost-effectiveness. The aim of this study was to evaluate the antibacterial effect of boron nitride (BN) and chitosan coated BN-Nps using different surfactants. In this regard, the potential antibacterial activity of prepared chitosan-coated and non-coated BN-Nps have been investigated against nine reference bacteria strains. BN-Nps and chitosan-coated BN-Nps were successfully developed and characterized. Nps determined that showed high zeta potential values (between -20.1 mV and +59.2 mV). Antimicrobial resistance results indicated that formulations of BN-Nps with negative zeta potential were found to be effective compared to chitosan-coated BN-Nps with high positive zeta potential. These findings emphasize the future availability of BN-Nps formulation providing antibacterial activity.

**Keywords:** antibacterial activity, boron nitride, chitosan, nanoparticles, zeta potential.

### Introduction

Nanotechnology offers the opportunity to design nanoparticles (Nps) that can be modified in composition, size, shape, and surface properties for application in medical fields.<sup>1</sup> Previous studies reported that Nps may enter viable cells using the cellular endocytosis mechanism such as phagocytosis and pinocytosis due to their resemblance to cellular components in size.<sup>2-4</sup>


In both prophylactic and therapeutic approaches, Nps can be used as a carrier system owing to their increased specific surface areas and functionality.<sup>5-7</sup> The efficiency, release kinetics,

and delivery pathways of the Nps can be altered by size, shape, surface charge, and hydrophobicity.<sup>8,9</sup>

Microbial infections are the primary source of chronic diseases and deaths. The multidrug-resistant bacteria including *Escherichia coli* (*E. coli*) and *Staphylococcus aureus* (*S. aureus*), are usually responsible for infections such as wounds, skin, and circulatory diseases. Antibiotics are the ideal treatment for bacterial infections due to their broad spectrum of practical results. However, many studies have reported that the widespread use and abuse of antibiotics have led to the emergence of multidrug-resistant bacteria, a significant weakness of current antibiotic therapy.<sup>10</sup> In addition, the selection of cyto-compatible agents during antimicrobial treatment applications increases the chance of success in treatment.<sup>11</sup> Therefore, the biocompatibility of Nps should be considered in the investigation of new agents as well as cost and antimicrobial effi-

<sup>#</sup>These authors equally contributed to this work.

<sup>†</sup>To whom correspondence should be addressed.

emrahozakar@atauni.edu.tr,  0000-0002-7443-208X

©2022 The Polymer Society of Korea. All rights reserved.

cacy. These are a glimmer of hope as they provide minimal death resistance compared to traditional antibiotics and anti-cancer drugs.<sup>12</sup> Many nanomaterials such as gold, silver, and graphene show excellent antimicrobial properties that can be used in various medicinal applications.<sup>13</sup>

Boron nitride (BN) is a potent compound formed by binding boron and nitrogen elements. Due to its crystal structure, it shows different physical and chemical properties.<sup>14-16</sup> BN has extraordinary and unique properties that provide a significant advantage in some special applications. Unlike graphene, BN has outstanding optical and mechanical properties, thermal conductivity, and a superior antioxidant capacity. Although adding carbon nanostructures to polymers can endanger electrical insulation, dielectric properties are preserved when BN is used.<sup>15,17</sup> Compared to its colored (primarily black) carbon-based counterparts, BN is white, and this feature allows it to be used in the medical field. Due to its superior properties and structure similar to those of carbon materials, BN can be used for applications ranging from the synthesis of composite materials to electrical and optical devices.<sup>15</sup> In addition, BN has been reported in the literature to show better biocompatibility, less toxicity, and more efficient intracellular uptake from carbon by cells.<sup>1,18</sup> Also, there are many cytotoxicity and biocompatibility studies on BN in the literature.<sup>15,19</sup>

Chitosan has essential properties such as biocompatible, biodegradable, and low toxicity.<sup>20</sup> Unlike other biodegradable polymers, chitosan is a polymer with cationic charge.<sup>18</sup> The electrostatic interaction occurs between the positive group (amine) of chitosan and the negative group of the other molecule. The size and surface charges of Nps can be changed by manipulating the quantity or molecular weight of chitosan. In this way, interaction with cells in the target region can be increased.<sup>21</sup> In the literature, there are antibacterial studies on chitosan in the form of beads, films, fibers, membranes, and hydrogels.<sup>22</sup> Also wound healing,<sup>23</sup> antimicrobial textile products<sup>24</sup> and food packaging products<sup>25</sup> have been reported by researchers by nano-based system studies conducted within the scope of the antibacterial activity of chitosan.

The nanoprecipitation technique is a fast and straightforward nanoparticle preparation technique and requires minimum equipment. It has an essential advantage in exhibiting a narrow particle size distribution in the preparation of BN-Nps formulation.<sup>26,27</sup> Also, positively charged chitosan can be used as a drug delivery system providing long-term and/or controlled release owing to its superior properties by the nanoprecipitation technique.<sup>28</sup>

This study aimed to evaluate the effect of BN, chitosan, and excipients used on the antibacterial effect of BN-Nps, which have not been reported yet. In this regard, the potential antibacterial activity of prepared chitosan-coated and non-coated BN-Nps has been investigated against nine reference bacteria strains. Additionally, characterizations of Nps were made, and their colloidal stability was also evaluated. In this study, for the first time in the literature, significant changes in the antimicrobial activities and, nanoparticle properties of the formulations were observed by changing the surfactants.

## Experimental

**Material.** Medium molecular weight chitosan, BN, Poloxamer 407, and high molecular weight (H-MW) polyvinyl alcohol (PVA) were purchased from Sigma-Aldrich, USA. Tween 20 and low molecular weight (L-MW) PVA were purchased from Merck, Germany. Acetic acid were purchased from Sigma, Germany. Mueller Hinton (MH) agar and MH broth were purchased from Oxoid, Basingstoke, United Kingdom. All chemicals used were of analytical or pharmaceutical grade. Ultrapure water was used in all analysis and studies (Merck Millipore Direct-Q™ 3, Germany).

**Development of BN-Nps and Chitosan-Coated BN-Nps Formulation.** Formulations have been developed using the 'Nanoprecipitation' technique (Figure 1).<sup>29</sup> Firstly, BN-Nps were prepared and then coated with chitosan. For this, 125 mg BN and 100 mg Tween 20 as a surfactant were dissolved in a vial containing 1 mL DMSO. After that, this solution was added into the aqueous phase containing 50 mg surfactant (Poloxamer 407 or PVA) and sonicated for 5 min into an ultrasonic bath (2-8 °C). Later, the supernatant was removed by ultracentrifugation (Kubota 3780, Japan) at 12500 rpm for 30 min. Excess surfactants, acetic acid and DMSO were washed several times with the addition of 5 mL ultrapure water and removed by ultracentrifugation at 12500 rpm for 10 min. Finally, obtained BN-Nps were suspended with the addition of 2 mL distilled water and lyophilized for 24 hours after being frozen at -20 °C overnight. For subsequent analyses, dry powder of BN-Nps was stored in a dark place in a desiccator at room temperature. The chitosan-coated BN-Nps were prepared in the same manner as described above, with the addition of chitosan before the ultracentrifugation step during the preparation of the BN-Nps.<sup>18</sup> In a vial, 62.5 or 125 mg chitosan was dissolved in the solution containing 1 mL 1% w/v acetic acid. Then, BN-Nps were added to this solution, and they were

coated with chitosan, as seen in Figure 1. After stirring for 2 hours, the supernatant was removed by ultracentrifugation at 12500 rpm for 30 min. Excess surfactants, acetic acid and DMSO were washed several times with the addition of 5 mL ultrapure water and removed by centrifuging at 12500 rpm for 10 min. The obtained chitosan-coated BN-Nps were suspended with 2 mL distilled water and frozen at  $-20\text{ }^{\circ}\text{C}$  overnight, then lyophilized for 24 hours (Martin Christ Alpha 1-4 Ldplus, Germany). For subsequent analyses, dry powder of chitosan-coated BN-Nps was stored in a dark place in a desiccator at room temperature.

**Characterization of Nps. Yield, Particle Size, Zeta Potential and Polydispersity Index (PDI) Analysis:** The amounts of all formulations were evaluated after lyophilization, and their yields were calculated by proportioning with the amount of material added in the initial phase ( $n=3$ ).<sup>29</sup>

The particle size, zeta potential, and PDI, measurements of the prepared BN-Nps and chitosan-coated BN-Nps formulations were determined by Zetasizer (Malvern Zetasizer Nano ZSP, UK) device. For this purpose, dilute samples of all formulations were prepared, and measurement was performed in at least three replicates for each formulation at room temperature.

**Scanning Electron Microscope (SEM) Analysis:** The morphology of lyophilized Nps formulations was analyzed to have an idea about the shape and average particle size distribution. Each Nps formulation was examined with SEM (Zeiss Sigma 300, Germany) device, and their images were taken. Since the formulations were non-conductive, they were coated with gold, approximately 100 Å thickness, for 20 seconds under vacuum.

**X-Ray Diffraction (XRD) Analysis:** XRD analysis is one of the characterization techniques used to detect changes in the crystal structure of the active substance.<sup>30</sup> X-ray diffractograms of pure substances and Nps were obtained by PANalytical Empyrean XRD (Netherlands) with Cu-K  $\alpha$  radiation ( $\lambda=1.541874\text{ \AA}$ ) conditioned at 45 kV and 40 mA. The  $2\theta$  range is between  $10\text{-}60^{\circ}$  with a scanning speed of  $2^{\circ}/\text{min}$ .<sup>31</sup>

**Fourier Transform Infrared (FTIR) Analysis:** This analysis was carried out to examine the interaction of pure substances, all formulations to be prepared, and all auxiliary substances to be used to prepare these formulations and determine whether there will be changes in the chemical structures of chitosan and BN in the formulations.<sup>32</sup> FTIR spectra of lyophilized formulations and pure substances were recorded from  $4000\text{ to }400\text{ cm}^{-1}$  at the resolution of  $4\text{ cm}^{-1}$  using an FTIR

spectrophotometer (Bruker VERTEX 70v, Germany) equipped with attenuated total reflection (ATR).

**Colloidal Stability of Nps:** During the evaluation of the antimicrobial activities of Nps formulations, their short-term colloidal stability was examined to observe the changes in size and zeta potentials during the incubation period.

Briefly, freshly prepared formulations suspended in pure water were re-analyzed in terms of zeta potential, PDI, and particle size at the end of 24 hours and 48 hours at  $25\pm 2^{\circ}\text{C}$  temperature and  $60\pm 5\%$  relative humidity.<sup>33</sup> All samples were stored in a dark place in the test tubes during colloidal stability tests.

**Assays for Antibacterial Activity of Nps Formulations:** *In vitro* antimicrobial activity of the prepared Nps with different concentrations and combinations was evaluated against reference bacterial strains including *Bacillus cereus* ATCC 10987 (*B. cereus*), *E. coli* ATCC 25922, *Enterococcus faecalis* ATCC 29212 (*E. faecalis*), *Klebsiella pneumoniae* ATCC 27736 (*K. pneumoniae*), *Pseudomonas aeruginosa* ATCC 27853 (*P. aeruginosa*), *Proteus mirabilis* ATCC 12453 (*P. mirabilis*), *Streptococcus agalactiae* ATCC 12986 (*S. agalactiae*), *S. aureus* ATCC 29213, and *Salmonella enterica subsp. enterica serovar Typhimurium* ATCC 14028 (*S. Typhimurium*). The bacteria were grown on MH agar for 24 hours at  $37\text{ }^{\circ}\text{C}$  to obtain a pure culture.

The minimum inhibitory concentration (MIC) was determined by a broth microdilution method (EUCAST, 2021). The initial concentration of the BN changed according to preparation methods (adjusted to min. 8 mg/mL and max. 12.5 mg/mL). Briefly, twofold serial dilutions of the Nps in a liquid solution were prepared in a 96-well microplate cation-adjusted MH broth. A bacterial inoculum was prepared at a density of 0.5 McFarland standard from an overnight growth of fresh

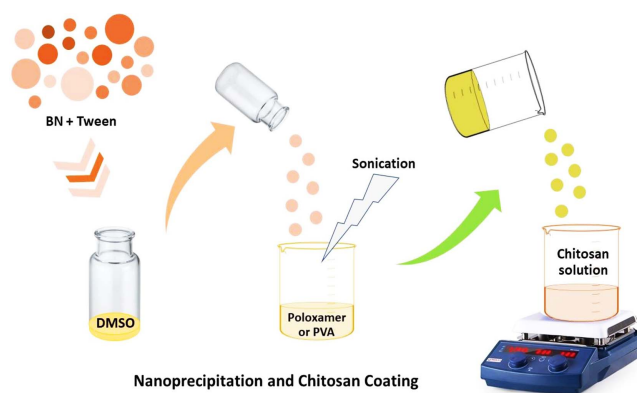


**Figure 1.** Preparation process of BN-Nps and chitosan coating.

bacterial culture in MH broth, diluted to 1:100 with MH broth, and distributed to the wells in 50  $\mu$ L volumes. The microplate was covered with the lid and incubated for 24 hours at 37 °C. At the end of the incubation, the plate was evaluated by optical density at a wavelength of 600 nm (OD600) using an ELISA reader apparatus (BioTek, Power Wave XS2, Germany).

The results compared with the negative control (including either MH broth or MH broth and bacteria) that included in the last two wells on the plate. MIC test has been repeated three times for each formulation.

**Thermogravimetric Analysis (TGA):** TGA analysis was performed using a thermogravimetric analyzer (Hitachi, STA 7300, Japan). It was studied with exactly 10 mg weighed accurately of coated BN Nps (B2 and B3). They were analyzed by heating to 1000 °C at a heating rate of 10 °C/min in nitrogen-air medium.<sup>34</sup>

**Statistical Analysis:** All acquired data were expressed as mean $\pm$ standard deviation ( $\bar{X}\pm$ SD). Also, a one-way analysis of variance (ANOVA) was performed to detect the zeta potential, PDI, size, colloidal stability, and MIC analysis differences between the formulations by IBM SPSS Statistics 20. A probability “P” of less than 0.05 was considered as statistically significant.

## Results and Discussion

**Development of BN-Nps and Chitosan-Coated BN-Nps Formulation.** The obtained Nps and their contents resulting from the formulation development studies were given in Table 1. Optical microscope images of the BN-Nps (B1) and

**Table 1. Formulations and Their Contents**

Formulation code	Formulation contents (mg)					
	BN	Chitosan	Tween 20	Poloxamer 407	PVA**	PVA*
B1	125	-	100	50	-	-
B2	125	62.5	100	50	-	-
B3	125	125	100	50	-	-
B4	125	-	100	-	50	-
B5	125	62.5	100	-	50	-
B6	125	125	100	-	50	-
B7	125	-	100	-	-	50
B8	125	62.5	100	-	-	50
B9	125	125	100	-	-	50

\*L-MW PVA, \*\*H-MW PVA

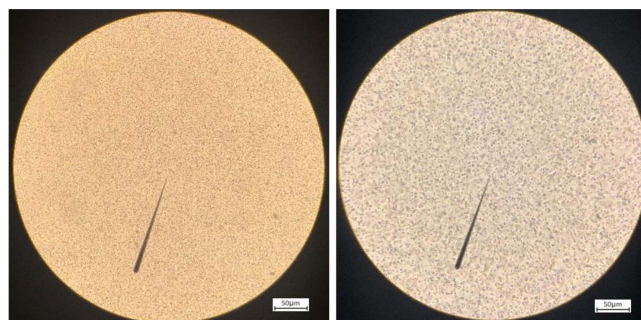


**Figure 2.** Optical microscope images of the B1 (left) and B2 (right), (magnification power 100 $\times$ ).

chitosan-coated BN-Nps (B2) were presented in Figure 2.

BN with a low dielectric constant is chemically inert and has very good mechanical resistance. BN is used in composite materials, accumulators, and insulating surfaces just like graphene. It is useful for biomedical applications due to its structural similarity to graphene. Also, BN-polymer composites are beneficial for biomedical devices and reduce associated infections. BN nanostructure has attracted a lot of attention recently due to these unique properties.<sup>35</sup> Although BN is used in nanodevices, composites, accumulators, and insulating surfaces, its use in biomedical applications is increasing due to its structural similarity with graphene.<sup>35,36</sup>

**Characterization of Nps. Yield, Particle Size, Zeta Potential and PDI Analysis:** The yield, particle size, zeta potential, and PDI data of prepared BN-Nps and chitosan-coated BN-Nps were given in Table 2. It has been observed smaller particles have been shown to have greater antibacterial activity against Gram-positive and Gram-negative bacteria. Similar results were found in studies in the literature.<sup>37</sup> However, a study indicated that larger particles could somehow reach into the bacterial cells and perform antimicrobial activity against *E. coli* as a model for Gram-negative bacteria.<sup>38</sup> This finding has mentioned the interaction of Nps with bacteria. With the increase in Nps size, bacterial interaction may improve depending on the growing surface.

Particles prepared with hydrophobic polymers undergo phagocytosis more easily than hydrophilic formulations. Considering the surface charge of particles, both anionic and cationic particles are taken up by cells. However, it has been reported that cationic particles escape from lysosomes.<sup>8</sup> Generally, membranous epithelial cells (M cells) take up particles of variable sizes from less than 1  $\mu$ m in size to over 5  $\mu$ m.

Particles smaller than 1  $\mu$ m are transferred to the basal medium, while particles larger than 5  $\mu$ m are sent to Peyer's

**Table 2. Yield, Particle Size, Zeta Potential, and PDI Measurement Data of Nps (n=3,  $\bar{X}\pm$ SD)**

	B1	B2	B3	B4	B5	B6	B7	B8	B9
Yield (%)	84.12 $\pm$ 3.51 <sup>a</sup>	90.37 $\pm$ 7.21 <sup>d</sup>	90.00 $\pm$ 7.55 <sup>g</sup>	85.58 $\pm$ 8.14 <sup>b</sup>	87.21 $\pm$ 6.11 <sup>d</sup>	88.58 $\pm$ 3.51 <sup>g</sup>	80.73 $\pm$ 4.58 <sup>c</sup>	88.89 $\pm$ 6.24 <sup>d</sup>	91.58 $\pm$ 6.43 <sup>g</sup>
Particle size (nm)	552.3 $\pm$ 6.97 <sup>a</sup>	1203 $\pm$ 17.04 <sup>d</sup>	1929 $\pm$ 24.01 <sup>g</sup>	458.6 $\pm$ 13.49 <sup>b</sup>	1558 $\pm$ 41.04 <sup>e</sup>	3100 $\pm$ 135.4 <sup>h</sup>	709.4 $\pm$ 38.88 <sup>c</sup>	1494 $\pm$ 12.01 <sup>d</sup>	2324 $\pm$ 37.72 <sup>i</sup>
Zeta potential (mV)	-20.1 $\pm$ 0.68 <sup>a</sup>	59 $\pm$ 1.14 <sup>d</sup>	48.4 $\pm$ 0.61 <sup>g</sup>	-12.8 $\pm$ 0.2 <sup>b</sup>	55.6 $\pm$ 1.54 <sup>e</sup>	43.9 $\pm$ 0.92 <sup>h</sup>	-7.75 $\pm$ 0.23 <sup>c</sup>	59.2 $\pm$ 0.31 <sup>d</sup>	53.8 $\pm$ 1.1 <sup>i</sup>
PDI	0.266 $\pm$ 0.03 <sup>a</sup>	0.337 $\pm$ 0.04 <sup>d</sup>	0.299 $\pm$ 0.05 <sup>g</sup>	0.205 $\pm$ 0.01 <sup>a</sup>	0.352 $\pm$ 0.06 <sup>d</sup>	0.288 $\pm$ 0.03 <sup>g</sup>	0.277 $\pm$ 0.08 <sup>a</sup>	0.260 $\pm$ 0.01 <sup>e</sup>	0.290 $\pm$ 0.04 <sup>g</sup>

<sup>a,b,c</sup>The statistical difference between B1, B4, B7 formulations bearing different symbols on the same line is significant (P<0.05).

<sup>d,e,f</sup>The statistical difference between B2, B5, B8 formulations bearing different symbols on the same line is significant (P<0.05).

<sup>g,h,i</sup>The statistical difference between B3, B6, B9 formulations bearing different symbols on the same line is significant (P<0.05).

patches. Negatively charged and hydrophobic Nps are advantageous as they undergo optimal absorption by M cells.<sup>39,40</sup> In addition, it has been reported that smaller particles were taken up more efficiently by alveolar macrophages.<sup>9</sup> In our study, the BN-Nps and chitosan-coated BN-Nps we obtained in our study were successfully prepared with very high yields. The yields were found to be between 80.73 $\pm$ 4.58-91.58 $\pm$ 6.43%. The yields of BN-Nps obtained in our study were compared, and the yields of BN-Nps (B1 and B4) prepared with Poloxamer 407 and high molecular weight PVA were similar. There was not found statistical difference between them (P>0.05). However, the yield of BN-Nps (B7) prepared with low molecular weight PVA was lower than B1 and B4. This result was statistically significant (P<0.05). This situation may be due to the excess of free BNs during nanoparticle formation due to the low molecular weight PVA forming a less steric barrier.<sup>41</sup> This situation may also be the case for chitosan-coated BN-Nps. Because BN-Nps were prepared first and then coated with chitosan.

The reason why B2, B3, B5, B6, B8, and B9 were obtained with higher efficiency compared to B1, B4 and B7 may be due to the chitosan's highly coating on the Nps surface. We can also understand this situation by the increased particle sizes in B2, B3, B5, B6, B8, and B9 compared to B1, B4, and B7. As the amount of chitosan increased, the yield did not change statistically, but the particle size increased significantly.

This case shows that the increased chitosan is covered with a thicker layer around the particle and increases the particle size.<sup>18</sup> Since the total amount of substance added and the final product's weight are compared when calculating the yield, we can say that chitosans are adsorbed to the surface in nanoparticle formation with a high density and therefore the yield loss is low. The sizes of Nps formulations prepared with only BN were found to be between 458-709 nm (Table 2; B1, B4, and B7). The size of Nps formulations coated with used chitosan in half the amount of BN increased 2-3 times compared to BN-

Nps (Table 2; B2, B5, and B8). The size of Nps formulations coated with used chitosan as much as the amount of BN increased 4-6 times (Table 2; B3, B6, and B9). This difference was statistically significant compared to the formulations not coated with chitosan (P<0.05). This situation showed a robust electrostatic interaction between chitosan's positive charges and BN's negative charges, and consequently, the size increased significantly (P<0.05). It has been reported that strong electrostatic interaction occurred due to the increase in negative charge density and the amount of chitosan, and consequently, the size increased in Nps systems.<sup>33</sup>

In the current study, the zeta potential of the BN-Nps by coating with chitosan was found between +43.9 mV and +59.2 mV. Although the zeta potential of pure BN-Nps was (-)mV, it was transformed to (+)mV in chitosan-coated BN-Nps complexes. Since physical stability is crucial in Nps, it has been reported that the zeta potential value >(±)60 mV is perfectly stable, ±40 to 60 mV is considered well stable, ±30 to 40 mV is considered stable, and <(±)30 mV is highly agglomerative.<sup>42,43</sup> Hence a physically stable formulation stabilized by electrostatic repulsion with a zeta potential of (±)30 mV is required as a minimum.<sup>44</sup> However, in the case of both electrostatic and steric stabilization, a zeta potential value of ±20 mV is sufficient.<sup>45</sup> These findings suggest that the chitosan coated the surface of BN-Nps and changed the zeta potential. These changes in the zeta potential were thought to be due to the presence of amino groups in the structure of the chitosan polymer.<sup>1</sup>

In our study, BN-Nps (see Figure 2) which were spherical, had a negative surface charge. In addition, their zeta potential values were in the range of -7.75 mV to -20.1 mV depending on the difference of surfactants used during the preparation. This zeta potential difference between formulations was statistically significant (P<0.05). With the dominance of negative charges due to the nature of BN, the zeta potential value of Nps reached up to -20.1 mV. Zeta potentials of BN-Nps

approached neutral, which was as expected, especially with the effect of cationic properties (PVA) of surfactants used (B4 and B7 in Table 2). However, with negative character surfactants such as Poloxamer 407, the zeta potential values of BN-Nps had higher negative values ( $P < 0.05$ ). Due to the increase in cationic charge with chitosan, the negative zeta potentials of BN-Nps had changed predominantly positively.

The PDI is an essential parameter in determining the long-term stability of nano-formulations. PDI value of 0.1-0.25 indicates a narrow particle size distribution, while a PDI value greater than 0.5 indicates an extensive size distribution.<sup>46,47</sup> It was observed that PDI values of all prepared formulations in the current study were around 0.2-0.3, and narrow size distribution in a homogeneous structure was realized and coating with chitosan did not change this situation. It was also obtained smaller particle size (458-709 nm) with BN-Nps and larger particle size (1203-3100 nm) with chitosan-coated BN-Nps.

**XRD Analysis:** XRD analysis was performed to examine the crystal structures of BN, chitosan, BN-Nps, and chitosan-coated BN-Nps and to detect changes in the crystal lattices in the structure (see Figure 3). For this purpose, diffractograms of pure BN, BN-Nps (B1), pure chitosan, and chitosan-coated

BN-Nps (B2) were taken.

The XRD diffractogram of chitosan showed that it had characteristic crystalline peaks around  $2\theta = 20^\circ$  (see Figure 3). It has been reported that the peaks around  $10^\circ$  and  $20^\circ$  are associated with crystal (1) and crystal (2) in chitosan, respectively.<sup>48,49</sup> BN is characterized by a long sharp peak at  $2\theta = 26-27^\circ$  and two minor peaks at  $2\theta = 41-42^\circ$  and  $55-56^\circ$ . BN-Nps formulations have displayed similar to the characteristic XRD diffractogram ( $2\theta = 26^\circ$ ,  $41^\circ$  and  $55^\circ$ ) of BN, and the crystalline structure was protected.<sup>48</sup> Although the crystal structure of the obtained nano-sized BNs with the using surfactants in the formulation was preserved, a slight decrease was observed in the peak intensities. This indicates that surfactants are located on the BN. In this way, we think that it creates a barrier layer on the particles to keep the BN at nanoscale. We predict that this layer also causes a decrease in the sharpness of the peaks.

The sharp peaks in Figure 3 of BN have decreased due to the coating with chitosan in the chitosan-coated BN-Nps diffractogram, the crystal structure is preserved. In addition, the characteristic crystalline peaks of chitosan  $19^\circ$  and characteristic crystalline peaks of BN  $27^\circ$ ,  $42^\circ$  and  $55^\circ$  were observed. These findings suggest that there was no change in the structure, and Nps were successfully obtained.<sup>48</sup>

**SEM Analysis:** SEM images of BN, chitosan, BN-Nps (B1), and chitosan-coated BN-Nps (B2) were presented in Figure 4. The SEM image results showed that the prepared BN-Nps dimensions from bulk material were compatible with the Zetasizer results ( $< 1 \mu\text{m}$ ), and the nanostructure had sharp lines. In addition, the chitosan-coated BN-Nps displayed that the sharp lines in the BN-Nps were smoother due to the increase in their size and the effect of the coating.

**FTIR Analysis:** FTIR analysis was performed to determine whether any undesired interactions or structure changes occurred during the formation of BN-Nps and chitosan-coated BN-Nps (Figure 5). For this purpose, spectra of pure BN, BN-Nps (B1), pure chitosan, and chitosan-coated BN-Nps (B2) were taken.

The FTIR spectrum of BN showed that the typical stretching vibration bands of the B-N bond and B-N-B bending vibration were associated around the spectral region of  $\sim 1340 \text{ cm}^{-1}$  and  $\sim 750 \text{ cm}^{-1}$  as previously reported.<sup>12,14,50,51</sup> The FTIR spectrum result of chitosan displayed that IR bands at the range of  $\sim 3400-3300 \text{ cm}^{-1}$  may be associated with the fact that was stretching bands of the -OH and primary amine groups (see Figure 5).

The characteristic IR peaks at  $\sim 1640 \text{ cm}^{-1}$ , and  $\sim 1580 \text{ cm}^{-1}$

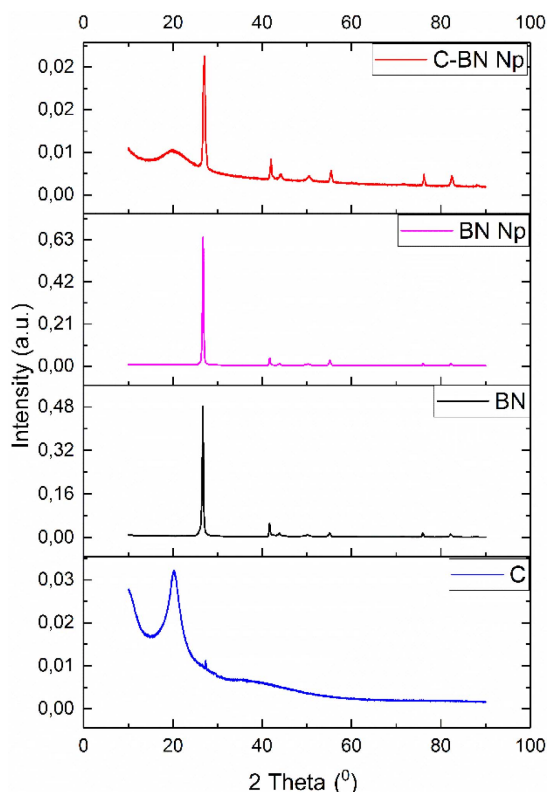


**Figure 3.** X-ray diffractogram of formulations and pure substances (C-BN-Np: B2, BN-Np: B1, BN: Boron nitride, C: Chitosan).

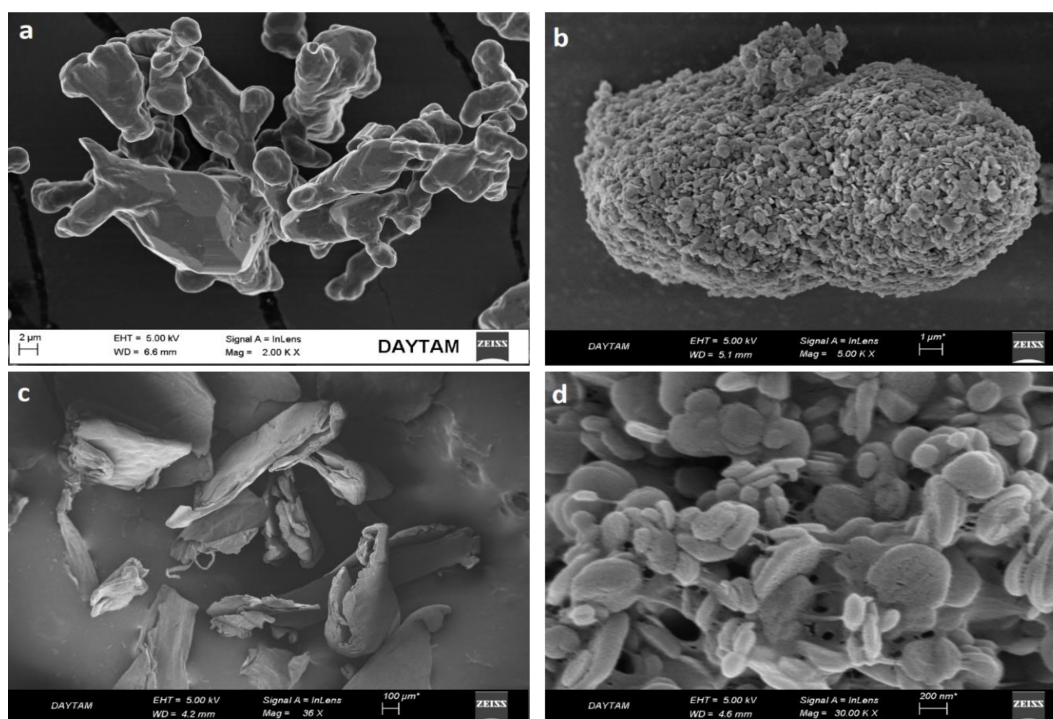


**Figure 4.** SEM images of (a) BN; (b) BN-Nps; (c) chitosan; (d) chitosan-coated BN-Nps.

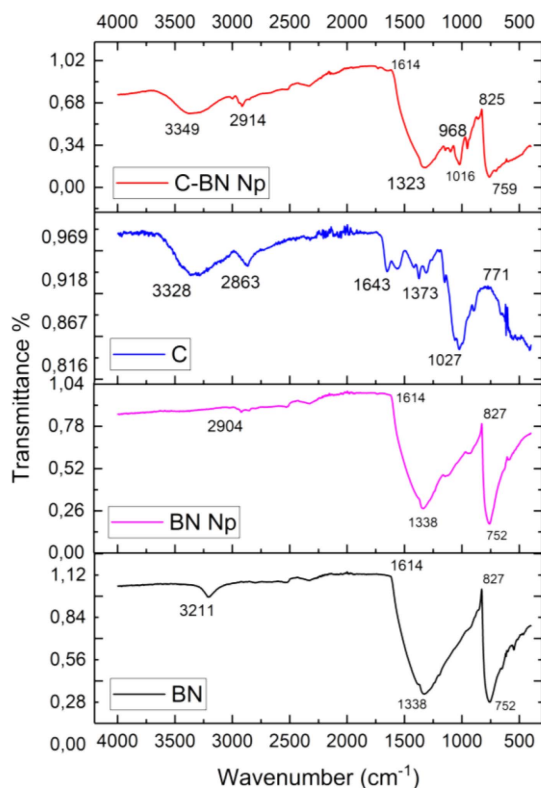


**Figure 5.** FTIR spectra of formulations and pure substances (C-BN-Np: B2, C: Chitosan, BN-Np: B1, BN: Boron nitride).

might be associated with the C-N and C=O stretching bands. As previously reported the C-H stretching bands were attributed to the bands at the spectral region of  $\sim 2860 \text{ cm}^{-1}$  and  $\sim 1370 \text{ cm}^{-1}$ , respectively.<sup>48</sup> The result of the Nps spectra showed that characteristic peaks occurred at IR bands of both chitosan and BN. The shift of the C-H stretching band from  $3349 \text{ cm}^{-1}$  to  $3328 \text{ cm}^{-1}$  in chitosan may be due to the interaction with Nps. In addition, the C=O and C-N stretch bands around  $\sim 1640 \text{ cm}^{-1}$  and  $\sim 1580 \text{ cm}^{-1}$  in chitosan, respectively, disappeared within the band tensions of BN in the structure. The absorption bands of BN and chitosan showed slight shifts in Nps. The characteristic peaks of BN at  $\sim 1340 \text{ cm}^{-1}$  and  $\sim 750 \text{ cm}^{-1}$  were also observed in BN-Nps. Besides, many IR stretching bands in the pure BN and chitosan were conserved during the formation of Nps without observing any chemical association or interaction. Therefore, the FTIR spectrum results showed that both BN and chitosan retained their structural integrity in Nps as in the XRD analysis. The presence of characteristic peaks of BN and chitosan in chitosan-coated BN-Nps in the current study indicated to be associated with the successful formation of Nps.<sup>12,18,48</sup> These findings suggest that the negatively charged BN-Nps were able to bind electrostatically to positively charged chitosan.<sup>18</sup>

**Colloidal Stability of Nps:** The short-term colloidal sta-

**Table 3. Colloidal Stability of Formulations (n=3,  $\bar{X}\pm$ SD)**

	Time	B1	B2	B3	B4	B5	B6	B7	B8	B9
Particle size (nm)	24h	562.1±6.42	1255±11.63	1955±9.02	463.5±4.23	1605±10.61	3223±61.12	761.4±9.92	1555±12.75	2349±42.41
	48h	564.9±8.14	1323±9.24	1981±10.32	465±4.91	1648±18.72	3280±69.55	781.9±19.02	1597±23.22	2341±31.86
Zeta potential (mV)	24h	-16.4±0.88	58.7±1.22	47.6±1.16	-12.6±0.22	54±1.22	42±2.01	-3.48±0.43	58.3±1.58	51.7±1.17
	48h	-16.2±0.78	57.3±1.41	47.1±0.79	-12.3±0.12	53.2±2.08	40.4±1.64	-2.99±1.31	57.8±2.42	50.4±1.57
PDI	24h	0.334±0.18	0.307±0.44	0.282±0.21	0.147±0.11	0.284±0.31	0.237±0.37	0.372±0.15	0.316±0.19	0.337±0.41
	48h	0.300±0.22	0.291±0.28	0.210±0.18	0.125±0.09	0.276±0.31	0.369±0.27	0.378±0.16	0.485±0.14	0.415±0.30

bilities of developed BN-Nps and chitosan-coated BN-Nps were given in Table 3.

The colloidal stability results were compared to the freshly prepared formulations as previously reported by a group of researchers.<sup>33</sup>

The results displayed that all formulations' zeta potential, particle size, and PDI values were stable throughout their incubation process with bacteria (see Table 3). B1 and B7 Nps had increased particle size and decreased zeta potential, which may be indicating a weak steric stabilization due to using the Poloxamer 407 and L-MW PVA (Table 3). This difference was significant compared to freshly prepared formulations ( $P<0.05$ ). It was observed that BN-Nps coated with chitosan provided excellent steric stabilization for 48 hours. A very slight zeta potential reduction may also be due to BN desorption from chitosan as described similarly in the previous study.<sup>33</sup>

**Evaluation of Antimicrobial Properties of Nps Formulations:** Antibacterial activity depends on the shape and size of the material, binding to bacteria, and also surface energy.<sup>52</sup> Several

experimental studies have been reported in the literature that 10 mm long BN nanosheets exhibit zero cytotoxicity and highlight their biocompatibility with kidneys.<sup>53</sup> Biocompatibility performance with cytotoxicity and cell viability assays varies depending on BN concentration and exposure time.<sup>1,54</sup>

The MIC results of the prepared Nps in this study were evaluated by the broth microdilution method and the results were given in Table 4. The MIC results changed with the selected Nps, which depends on the surfactants and chitosan amounts used during preparation. As shown in Table 4, MIC values of the B2 Nps formulation did not have an antimicrobial activity to *B. cereus*, *E. coli*, *E. faecalis* and *K. pneumonia*. All other formulations (except B3) had reasonably good MIC results against all microorganisms studied, indicating that our formulations have good antimicrobial activity.<sup>55</sup> In addition, some formulation of Nps prepared in the current study included chitosan to form the combination of negative and positive charges of BN-Nps.

The MIC results of B1 and B7 formulations had antibacterial

**Table 4. The MIC Results of Tested Microorganisms Against to Prepared BN-Nps and Chitosan-Coated BN-Nps**

Microorganisms	MIC results (dilution range, mg/mL)								
	B1 (10 to 0.02)	B2* (8 to 0.01)	B3** (8 to 0.01)	B4 (12.5 to 0.02)	B5* (8 to 0.01)	B6** (8 to 0.01)	B7 (12.5 to 0.02)	B8* (8 to 0.01)	B9** (8 to 0.01)
<i>B. cereus</i>	0.625 <sup>a</sup>	-	0.5 <sup>g</sup>	3.1 <sup>b</sup>	0.5 <sup>d</sup>	0.5 <sup>g</sup>	0.4 <sup>c</sup>	0.5 <sup>d</sup>	1 <sup>g</sup>
<i>E. coli</i>	0.625 <sup>a</sup>	-	-	3.1 <sup>b</sup>	1 <sup>d</sup>	1 <sup>g</sup>	0.4 <sup>c</sup>	1 <sup>d</sup>	4 <sup>h</sup>
<i>E. faecalis</i>	0.625 <sup>a</sup>	-	0.5 <sup>g</sup>	0.4 <sup>b</sup>	0.5 <sup>d</sup>	0.5 <sup>g</sup>	0.4 <sup>b</sup>	2 <sup>e</sup>	4 <sup>h</sup>
<i>K. pneumonia</i>	2.5 <sup>a</sup>	-	2 <sup>g</sup>	1.6 <sup>b</sup>	1 <sup>d</sup>	1 <sup>h</sup>	3.1 <sup>c</sup>	2 <sup>d</sup>	2 <sup>i</sup>
<i>P. aeruginosa</i>	2.5 <sup>a</sup>	2 <sup>d</sup>	-	1.6 <sup>b</sup>	2 <sup>d</sup>	4 <sup>g</sup>	3.1 <sup>c</sup>	2 <sup>d</sup>	4 <sup>g</sup>
<i>P. mirabilis</i>	1.25 <sup>a</sup>	0.5 <sup>d</sup>	0.5 <sup>g</sup>	0.4 <sup>b</sup>	0.5 <sup>d</sup>	0.5 <sup>g</sup>	1.6 <sup>c</sup>	1 <sup>d</sup>	2 <sup>h</sup>
<i>S. agalactiae</i>	1.25 <sup>a</sup>	0.25 <sup>d</sup>	0.25	0.8 <sup>b</sup>	0.5 <sup>e</sup>	0.5	3.1 <sup>c</sup>	0.25 <sup>d</sup>	2
<i>S. aureus</i>	1.25 <sup>a</sup>	0.25 <sup>d</sup>	0.25 <sup>g</sup>	0.4 <sup>b</sup>	0.25 <sup>d</sup>	0.5 <sup>g</sup>	1.6 <sup>c</sup>	2 <sup>e</sup>	4 <sup>h</sup>
<i>S. Typhimurium</i>	1.25 <sup>a</sup>	0.5 <sup>d</sup>	0.2 <sup>g</sup>	0.8 <sup>b</sup>	1 <sup>d</sup>	1 <sup>h</sup>	1.6 <sup>c</sup>	2 <sup>d</sup>	2 <sup>h</sup>

\*BN-Nps coated with 62.5 mg chitosan; \*\*BN-Nps coated with 125 mg chitosan

<sup>a,b,c</sup>The statistical difference between B1, B4, B7 formulations bearing different symbols on the same line is significant ( $P<0.05$ ).

<sup>d,e,f</sup>The statistical difference between B2, B5, B8 formulations bearing different symbols on the same line is significant ( $P<0.05$ ).

<sup>g,h,i</sup>The statistical difference between B3, B6, B9 formulations bearing different symbols on the same line is significant ( $P<0.05$ ).



activity against *E. coli* at a much lower concentration than previously reported by researchers.<sup>12,55-57</sup> The non-coated BN-Nps (B1 and B7) prepared in the current study were more effective against *B. cereus*, *E. coli*, and *E. faecalis* when compared to chitosan-coated BN-Nps formulations (B2, B3, B5, B6, B8, and B9) ( $P < 0.05$ ). Interestingly, the MIC results of B2, B5, and B8 formulations (containing 4 mg/mL chitosan) against *P. aeruginosa* displayed higher antimicrobial activity than the other chitosan-coated BN-Nps (containing 8 mg/mL chitosan) formulations. B4 formulation was the most effective against *P. aeruginosa* among all formulations. This may be due to the smallest size (458.6 nm) of B4 among all formulations, and therefore size can be said to be important in its interaction with *P. aeruginosa*.

For *S. agalactiae*, MIC results did not change with the increase in the amount of chitosan, but BN-Nps coated with chitosan were statistically significantly more effective than formulations containing only BN.

Overall, formulation B9 was the least effective against *E. coli*, *E. faecalis*, *P. aeruginosa*, *P. mirabilis*, *S. aureus*, and *S. Typhimurium* among all formulations. The reason for this situation may be that it was prepared with L-MW PVA, which could not provide sufficient steric stabilization against the increased amount of chitosan. The prepared formulations with Poloxamer 407 (B2 and B3) were found to be more effective against *S. aureus*. B2, B5, and B8 formulations (containing 4 mg/mL chitosan) had higher antimicrobial activity, whereas B3, B6, and B9 formulations (containing 8 mg/mL chitosan) had lower. Increasing size depending on the amount of chitosan added is an essential parameter in interacting with bacteria.

The positively charged Nps (B2, B3, B5, B6, B8, B9) showed antimicrobial activity against tested bacteria as expected. Similarly, it has been reported that positively charged Nps displayed vigorous antimicrobial activity against *E. coli* compared to the negatively charged formulations.<sup>38</sup> Another study indicated that although negatively charged silver Nps showed deficient antibacterial activity, positively charged and neutral silver Nps had higher antibacterial activity against Gram-positive and Gram-negative bacteria.<sup>37</sup> Contrary to previous studies, in this study, surprisingly, B1, B4, and B7 with negative zeta potential were found to show much more antimicrobial activity against most tested bacteria, such as *S. agalactiae* and *S. aureus*, according to the MIC results. Thus, we found that negatively charged formulations showed higher antimicrobial activity. Indeed, there are differences in the membrane structures of

Gram-positive and Gram-negative bacteria, most of them have a negative surface charge at physiological pH values.<sup>38,58</sup> It is known that both Gram-positive and Gram-negative bacteria interact with positively charged particles much more easily through electrostatic attraction than with negatively charged particles.<sup>58,59</sup> The cell membrane in Gram-positive bacteria consists mainly of a thick layer of peptidoglycan with embedded teichoic acid. On the other hand, Gram-negative bacteria have a lipopolysaccharide layer on their outer surface followed by a thin peptidoglycan layer. Teichoic acid and lipopolysaccharides impart a negative charge to the surface of bacterial cells.<sup>60</sup>

**TGA Analysis:** The TGA thermogram of chitosan-coated BN-Nps (B2 and B3) were given in Figure 6. The TGA analysis results were compared to the pure BN and pure chitosan as previously reported by various of researchers. The TGA was used to evaluate the thermal stabilities of chitosan-coated BN Nps. As shown in Figure 6, the initial decomposition temperature of the NPS's was about 190-200 °C. The addition of chitosan has no effect on the major decomposition process of the BN. The interaction of BN with the chitosan increased the thermal resistance of the Nps and, consequently, the thermal decomposition temperature. These indicators were consistent with similar studies in the literature.<sup>48,61,62</sup>

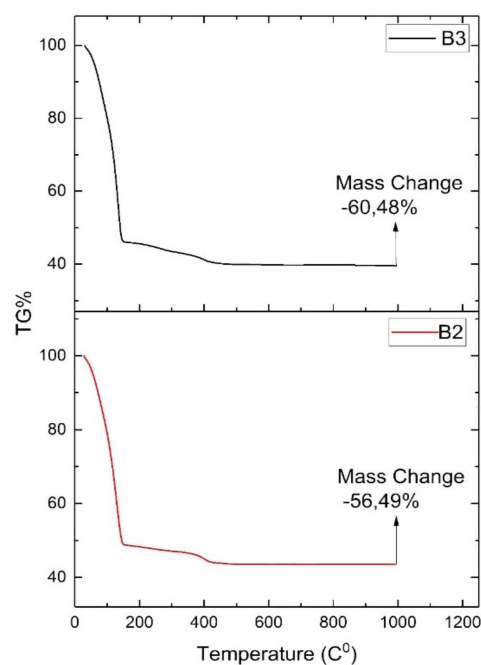


**Figure 6.** TGA curve of chitosan-coated BN-Nps (B3 and B2; Heating rate: 10 °C/min, Temperature range 25-1000 °C, under Nitrogen atmosphere).

Silver nanoparticles (Ag-NPs) have also been extensively researched in the literature due to their antibacterial properties.<sup>63</sup> The positive charge of AgNPs concerning their antimicrobial activity is thought to be due to the electrostatic attraction between negatively charged bacterial cells. Although there are differences in the membrane structures of Gram-positive and Gram-negative bacteria, most of them have a negative charge. AgNPs have been shown to be more active against gram-negative bacteria regardless of their resistance level. It has been reported that positively charged AgNPs are superior in antibacterial activity to negatively charged nanoparticles.<sup>37</sup> However, in our study, it was determined that both positively charged chitosan-coated BN Nps and negatively charged BN Nps showed antibacterial activity. It was observed here that it did not inhibit cells as a result of physical interaction with the bacterial cell wall, as in AgNp's.

It is widely accepted that high concentrations of AgNPs can induce apoptosis in human cells. AgNPs have been reported to exhibit higher cytotoxicity than silver microparticles, with signs such as more severe morphological abnormalities and more cells undergoing apoptosis. This indicates that the in vitro cytotoxicity mechanism of AgNPs is related to their nano size. Silver ions bind to proteins and nucleic acid and interfere with cell functions. Intracellular reactive oxygen species (ROS) production by AgNPs has been clearly detected. The general view is that mitochondrial damage is the basis of AgNP-induced early apoptosis mechanism. Chromosomal abnormalities directly result from DNA damage, such as double-strand breaks and intact strand breaks, resulting in the chromosomal rearrangement. AgNPs can access the mitochondria to interfere with the respiratory chain, resulting in the presence of a large number of superoxide and nano-silver ions that can damage the cell nucleus, genetic material, and other structural organelles.<sup>64,65</sup>

Orally ingested AgNPs accumulate permanently in the body, both as AgNp and as released Ag<sup>+</sup> ions, and 2-4% of the absorbed silver is retained in the tissues. The most visible consequences of prolonged exposure to silver are "Argyria," an irreversible bluish skin pigmentation due to silver deposition. In addition to Argyria, numerous studies have identified multiple side effects and toxicity in various organs based on AgNP exposure. Although silver is found in small amounts in the human body, it does not have a physiological function. It is not an essential element in the body.<sup>66</sup>

However, boron is a metalloid that plays an important role in the functioning of the cell membrane of animals, enzymatic

reactions, hormonal and mineral metabolism. Boron is also thought to be an essential metalloid for animals. Boron does not accumulate in soft tissues; however, it accumulates efficiently in the bones. Boron affects skeletal metabolism. Therefore, it affects bone growth and compositional properties of soft tissues in animals and humans. Boron-rich diets have a positive impact on calcification and preservation of mammalian bones, and central nervous system functions and also play a positive role in maintaining the structural integrity and function of cell membranes. More than 90% of excess borate in mammals is excreted as boric acid in the urine.<sup>67</sup> In a study, the researchers reported that ROS, cellular changes, or apoptosis were not observed by day 9.<sup>12</sup>

There are limited antibacterial studies conducted with BN nanoparticles and/or chitosan-added BN in the literature. This study was designed based on the antibacterial properties of BN nanoparticles reported in the literature. With the effect of different surfactants and varying amounts of chitosan, the antimicrobial activities of BN nanoparticles on 9 different bacterial species were examined, and the surprising results were shared with the scientific world. Further analysis is needed to definitively ascertain the exact mechanism under the antimicrobial activity of the negatively charged Nps formulations. This situation will inspire both us and the other scientists for further studies. In the light of all these comparative data, we hope to see the frequency of biomedical applications of BN-containing nanomaterials more in the future.

## Conclusions

In summary, the nine different formulations were developed and characterized, and their results and antimicrobial activities were examined and discussed in terms of formulation components, zeta potential, and particle size changes. The morphology of the prepared Nps was determined by an optical microscope and SEM. As a result of the analyzes made with FTIR and XRD, undesirable interactions were not found in their structures. The findings from the current study further point out the effect of antimicrobial properties against nine reference bacteria of the BN-Nps and chitosan-coated BN-Nps. Surprisingly, BN-Nps with negative zeta potential (B1 and B7 formulation) showed antibacterial activity even at low concentrations, contrary to what previous researchers found. In addition, it has been determined that the antimicrobial activity decreases as the amount of chitosan coating increases in some bacteria (*P. aeruginosa*), but the increase in the amount of chi-

tosan coating is not significant for some bacterial species (*S. agalactiae*). In the future, our developed BN-Nps and chitosan-coated BN-Nps formulations may provide antibacterial activity even at low doses, making them safe and biocompatible for biological applications. In light of the data obtained this study, we think it is unique to find out which formulation component or which particle size or which zeta potential's is more effective against bacteria.

**Conflict of Interest:** The authors declare that there is no conflict of interest.

## References

- Ciofani, G.; Danti, S.; D'Alessandro, D.; Moscato, S.; Menciassi, A. Assessing Cytotoxicity of Boron Nitride Nanotubes: Interference with the MTT Assay. *Biochem. Biophys. Res. Commun.* **2010**, *394*, 405-411.
- Behzadi, S.; Serpooshan, V.; Tao, W.; Hamaly, M. A.; Alkawareek, M. Y.; Dreaden, E. C.; Brown, D.; Alkilany, A. M.; Farokhzad, O. C.; Mahmoudi, M. Cellular Uptake of Nanoparticles: Journey Inside the Cell. *Chem. Soc. Rev.* **2017**, *46*, 4218-4244.
- Rennick, J. J.; Johnston, A. P. R.; Parton, R. G. Key Principles and Methods for Studying the Endocytosis of Biological and Nanoparticle Therapeutics. *Nat. Nanotechnol.* **2021**, *16*, 266-276.
- Li, J.; Chen, C.; Xia, T. Understanding Nanomaterial-Liver Interactions to Facilitate the Development of Safer Nanoapplications. *Adv. Mater.* **2022**, *34*, 2106456.
- Hunsawong, T.; Sunintaboon, P.; Warit, S.; Thaisomboonsuk, B.; Jarman, R. G.; Yoon, I.-K.; Ubol, S.; Fernandez, S. Immunogenic Properties of a BCG Adjuvanted Chitosan Nanoparticle-Based Dengue Vaccine in Human Dendritic Cells. *PLoS Negl. Trop. Dis.* **2015**, *9*, e0003958.
- Kheirollahpour, M.; Mehrabi, M.; Dounighi, N. M.; Mohammadi, M.; Masoudi, A. Nanoparticles and Vaccine Development. *Pharm. Nanotechnol.* **2020**, *8*, 6-21.
- Zhao, L.; Seth, A.; Wibowo, N.; Zhao, C.-X.; Mitter, N.; Yu, C.; Middelberg, A. P. J. Nanoparticle Vaccines. *Vaccine* **2014**, *32*, 327-337.
- Maina, T. W.; Grego, E. A.; Boggiatto, P. M.; Sacco, R. E.; Narasimhan, B.; McGill, J. L. Applications of Nanovaccines for Disease Prevention in Cattle. *Front. Bioeng. Biotechnol.* **2020**, *8*.
- Silva, A. L.; Soema, P. C.; Slütter, B.; Ossendorp, F.; Jiskoot, W. PLGA Particulate Delivery Systems for Subunit Vaccines: Linking Particle Properties to Immunogenicity. *Hum. Vaccin. Immunother.* **2016**, *12*, 1056-1069.
- Fair, R. J.; Tor, Y. Antibiotics and Bacterial Resistance in the 21st Century. *Perspect. Medicin. Chem.* **2014**, *6*, PMC-S14459.
- Nur, A. R.; Yeit, H. T.; Ebrahim M. Current Approaches for the Exploration of Antimicrobial Activities of Nanoparticles. *Sci. Technol. Adv. Mater.* **2021**, *22*, 885-907.
- Mukheem, A.; Shahabuddin, S.; Akbar, N.; Miskon, A.; Muhamad Sarih, N.; Sudesh, K.; Ahmed Khan, N.; Saidur, R.; Sridewi, N. Boron Nitride Doped Polyhydroxyalkanoate/Chitosan Nanocomposite for Antibacterial and Biological Applications. *Nanomater.* **2019**, *9*, 645.
- Rabiee, N.; Ahmadi, S.; Akhavan, O.; Luque, R. Silver and Gold Nanoparticles for Antimicrobial Purposes Against Multi-Drug Resistance Bacteria. *Materials (Basel)*. **2022**, *15*, 1799.
- Kıvanç, M.; Barutca, B.; Koparal, A. T.; Göncü, Y.; Bostancı, S. H.; Ay, N. Effects of Hexagonal Boron Nitride Nanoparticles on Antimicrobial and Antibiofilm Activities, Cell Viability. *Mater. Sci. Eng. C*. **2018**, *91*, 115-124.
- Merlo, A.; Mokkaçpati, V. R. S. S.; Pandit, S.; Mijakovic, I. Boron Nitride Nanomaterials: Biocompatibility and Bio-Applications. *Biomater. Sci.* **2018**, *6*, 2298-2311.
- Semmah, A.; Heireche, H.; Bousahla, A. A.; Tounsi, A. Thermal Buckling Analysis of SWBNNT on Winkler Foundation by Non-Local FSDT. *Adv. Nano Res.* **2019**, *7*, 89.
- Joy, J.; George, E.; Haritha, P.; Thomas, S.; Anas, S. An Overview of Boron Nitride Based Polymer Nanocomposites. *J. Polym. Sci.* **2020**, *58*, 3115-3141.
- Zhang, H.; Chen, S.; Zhi, C.; Yamazaki, T.; Hanagata, N. Chitosan-Coated Boron Nitride Nanospheres Enhance Delivery of CpG Oligodeoxynucleotides and Induction of Cytokines. *Int. J. Nanomedicine.* **2013**, *8*, 1783.
- Zhang, H.; Feng, S.; Yan, T.; Zhi, C.; Gao, X.-D.; Hanagata, N. Polyethyleneimine-Functionalized Boron Nitride Nanospheres as Efficient Carriers for Enhancing the Immunostimulatory Effect of CpG Oligodeoxynucleotides. *Int. J. Nanomedicine.* **2015**, *10*, 5343.
- Fatullayeva, S.; Tagiyev, D.; Zeynalov, N. Samira M.; Elmira, A. Recent Advances of Chitosan-Based Polymers in Biomedical Applications and Environmental Protection. *J. Polym. Res.* **2022**, *29*, 259.
- Jabbal-Gill, I.; Watts, P.; Smith, A. Chitosan-Based Delivery Systems for Mucosal Vaccines. *Expert Opin. Drug Deliv.* **2012**, *9*, 1051-1067.
- Perinelli, D. R.; Fagioli, L.; Campana, R.; Lam, J. K. W.; Baffone, W.; Palmieri, G. F.; Casettari, L.; Bonacucina, G. Chitosan-Based Nanosystems and Their Exploited Antimicrobial Activity. *Eur. J. Pharm. Sci.* **2018**, *117*, 8-20.
- Sarhan, W. A.; Azzazy, H. M. E. High Concentration Honey Chitosan Electrospun Nanofibers: Biocompatibility and Antibacterial Effects. *Carbohydr. Polym.* **2015**, *122*, 135-143.
- Ibrahim, N. A.; El-Zairy, E. M.; Eid, B. M.; Emam, E.; Barkat, S. R. A New Approach for Imparting Durable Multifunctional Properties to Linen-Containing Fabrics. *Carbohydr. Polym.* **2017**, *157*, 1085-1093.
- Feyzioglu, G. C.; Tornuk, F. Development of Chitosan Nanoparticles Loaded with Summer Savory Essential Oil for Antimicrobial and Antioxidant Delivery Applications. *LWT Food Sci. Technol.* **2016**, *70*, 104-110.
- Liu, Y.; Yang, G.; Zou, D.; Hui, Y.; Nigam, K.; Middelberg, A. P. J.; Zhao, C.-X. Formulation of Nanoparticles Using Mixing-

- Induced Nanoprecipitation for Drug Delivery. *Ind. Eng. Chem. Res.* **2020**, *59*, 4134-4149.
27. Salatin, S.; Barar, J.; Barzegar-Jalali, M.; Adibkia, K.; Kiafar, F.; Jelvehgari, M. Development of a Nanoprecipitation Method for The Entrapment of a Very Water-Soluble Drug into Eudragit RL Nanoparticles. *Res. Pharm. Sci.* **2017**, *12*, 1-14.
  28. Yamamoto, H.; Kuno, Y.; Sugimoto, S.; Takeuchi, H.; Kawashima, Y. Surface-Modified PLGA Nanosphere with Chitosan Improved Pulmonary Delivery of Calcitonin By Mucoadhesion and Opening of the Intercellular Tight Junctions. *J. Control. Release.* **2005**, *102*, 373-381.
  29. Meewan, J.; Somani, S.; Almowalad, J.; Laskar, P.; Mullin, M.; MacKenzie, G.; Khadke, S.; Perrie, Y.; Dufès, C. Preparation of Zein-Based Nanoparticles: Nanoprecipitation versus Microfluidic-Assisted Manufacture, Effects of PEGylation on Nanoparticle Characteristics and Cellular Uptake by Melanoma Cells. *Int J Nanomedicine.* **2022**, *17*, 2809-2822.
  30. Mourdikoudis, S.; Pallares, R. M.; Thanh, N. T. K. Characterization Techniques for Nanoparticles: Comparison and Complementarity Upon Studying Nanoparticle Properties. *Nanoscale.* **2018**, *10*, 12871-12934.
  31. Barnabas, M. J.; Parambadath, S.; Nagappan, S.; Chung, I.; Ha, C.-S. Silver (I)-Schiff-Base Complex Intercalated Layered Double Hydroxide with Antimicrobial Activity. *Adv. Nano Res.* **2021**, *10*, 373-383.
  32. Sevinç Özakar, R.; Özakar, E. Different Biopolymers" Effects on the Evaluation and Characterization of Floating Tablets Prepared by Lyophilization Technique to Improve the Quality Control Parameters. *Polym. Korea* **2022**, *46*, 145-158.
  33. Rose, F.; Wern, J. E.; Gavins, F.; Andersen, P.; Follmann, F.; Foged, C. A Strong Adjuvant Based on Glycol-Chitosan-Coated Lipid-Polymer Hybrid Nanoparticles Potentiates Mucosal Immune Responses Against the Recombinant Chlamydia Trachomatis Fusion Antigen CTH522. *J. Control. Release.* **2018**, *271*, 88-97.
  34. Öner, M.; Kızıl, G.; Keskin, G.; Pochat-Bohatier, C.; Bechelany, M. The Effect of Boron Nitride on the Thermal and Mechanical Properties of Poly(3-hydroxybutyrate-co-3-hydroxyvalerate). *Nanomaterials.* **2018**, *11*, 940.
  35. Kayani, Z. N.; Bashir, Z.; Mohsin, M.; Riaz, S.; Naseem, S. Sol-Gel Synthesized Boron Nitride (BN) Thin Films for Antibacterial and Magnetic Applications. *Optik (Stuttg).* **2021**, *243*, 167502.
  36. Pandit, S.; Gaska, K.; Mokkaapati, V. R. S. S.; Forsberg, S.; Svensson, M.; Kádár, R.; Mijakovic, I. Antibacterial Effect of Boron Nitride Flakes with Controlled Orientation in Polymer Composites. *RSC Adv.* **2019**, *9*, 33454-33459.
  37. Abbaszadegan, A.; Ghahramani, Y.; Gholami, A.; Hemmateenejad, B.; Dorostkar, S.; Nabavizadeh, M.; Sharghi, H. The Effect of Charge at the Surface of Silver Nanoparticles on Antimicrobial Activity against Gram-Positive and Gram-Negative Bacteria: A Preliminary Study. *J. Nanomater.* **2015**, *2015*, 720654.
  38. Li, Z.; Ma, J.; Ruan, J.; Zhuang, X. Using Positively Charged Magnetic Nanoparticles to Capture Bacteria at Ultralow Concentration. *Nanoscale Res. Lett.* **2019**, *14*, 195.
  39. Mehrabi, M.; Montazeri, H.; Mohamadpour Dounighi, N.; Rashti, A.; Vakili-Ghartavol, R. Chitosan-based Nanoparticles in Mucosal Vaccine Delivery. *Arch. Razi Inst.* **2018**, *73*, 165-176.
  40. Shim, S.; Yoo, H. S. The Application of Mucoadhesive Chitosan Nanoparticles in Nasal Drug Delivery. *Mar. Drugs.* **2020**, *18*, 605.
  41. Lee, A.; Tsai, H.-Y.; Yates, M. Z. Steric Stabilization of Thermally Responsive N-Isopropylacrylamide Particles by Poly(vinyl alcohol). *Langmuir.* **2010**, *26*, 18055-18060.
  42. Ali, N.; Teixeira, J. A.; Addali, A. A Review on Nanofluids: Fabrication, Stability, and Thermophysical Properties. *J. Nanomater.* **2018**, *2018*, 6978130.
  43. Honary, S.; Zahir, F. Effect of Zeta Potential on The Properties of Nano-Drug Delivery Systems-A Review (Part 2). *Trop. J. Pharm. Res.* **2013**, *12*, 265-273.
  44. Koca, M.; Özakar, R. S.; Özakar, E.; Sade, R.; Pirimoğlu, B.; Özek, N. Ş.; Aysin, F. Preparation and Characterization of Nanosuspensions of Triiodoaniline Derivative New Contrast Agent, and Investigation into Its Cytotoxicity and Contrast Properties. *Iran. J. Pharm. Res.* **2022**, *21*, e123824.
  45. Singare, D. S.; Marella, S.; Gowthamrajan, K.; Kulkarni, G. T.; Vooturi, R.; Rao, P. S. Optimization of Formulation and Process Variable of Nanosuspension: An Industrial Perspective. *Int. J. Pharm.* **2010**, *402*, 213-220.
  46. Ali, H. S. M.; York, P.; Blagden, N. Preparation of Hydrocortisone Nanosuspension Through A Bottom-Up Nanoprecipitation Technique Using Microfluidic Reactors. *Int. J. Pharm.* **2009**, *375*, 107-113.
  47. Patravale, V. B.; Date, A. A.; Kulkarni, R. M. Nanosuspensions: A Promising Drug Delivery Strategy. *J. Pharm. Pharmacol.* **2004**, *56*, 827-840.
  48. Kisku, S. K.; Swain, S. K. Synthesis and Characterization of Chitosan/Boron Nitride Composites. *J. Am. Ceram. Soc.* **2012**, *95*, 2753-2757.
  49. Samuels, R. J. Solid State Characterization of the Structure of Chitosan Films. *J. Polym. Sci. Polym. Phys. Ed.* **1981**, *19*, 1081-1105.
  50. Salehirad, M.; Nikje, M. M. A. Synthesis and Characterization of Exfoliated Polystyrene Grafted Hexagonal Boron Nitride Nanosheets and Their Potential Application in Heat Transfer Nanofluids. *Iran. Polym. J.* **2017**, *26*, 467-480.
  51. Shahabuddin, S.; Khanam, R.; Khalid, M.; Sarih, N. M.; Ching, J. J.; Mohamad, S.; Saidur, R. Synthesis of 2D Boron Nitride Doped Polyaniline Hybrid Nanocomposites for Photocatalytic Degradation of Carcinogenic Dyes from Aqueous Solution. *Arab. J. Chem.* **2018**, *11*, 1000-1016.
  52. Ikram, M.; Jahan, I.; Haider, A.; Hassan, J.; Ul-Hamid, A.; Imran, M.; Haider, J.; Shahzadi, A.; Shahbaz, A.; Ali, S. Bactericidal Behavior of Chemically Exfoliated Boron Nitride Nanosheets Doped with Zirconium. *Appl. Nanosci.* **2020**, *10*, 2339-2349.
  53. Mateti, S.; Wong, C. S.; Liu, Z.; Yang, W.; Li, Y.; Li, L. H.; Chen, Y. Biocompatibility of Boron Nitride Nanosheets. *Nano Res.* **2018**, *11*, 334-342.
  54. Horváth, L.; Magrez, A.; Golberg, D.; Zhi, C.; Bando, Y.; Smajda,

- R.; Horváth, E.; Forró, L.; Schwaller, B. *In Vitro* Investigation of the Cellular Toxicity of Boron Nitride Nanotubes. *ACS Nano*. **2011**, 5, 3800-3810.
55. Maria Nithya, J. S.; Pandurangan, A.; Aqueous Dispersion of Polymer Coated Boron Nitride Nanotubes and Their Antibacterial and Cytotoxicity Studies. *RSC Adv*. **2014**, 4, 32031-32046.
  56. Firestein, K. L.; Leybo, D. V.; Steinman, A. E.; Kovalskii, A. M.; Matveev, A. T.; Manakhov, A. M.; Sukhorukova, I. V.; Slukin, P. V.; Fursova, N. K.; Ignatov, S. G. BN/Ag Hybrid Nanomaterials with Petal-Like Surfaces as Catalysts and Antibacterial Agents. *Beilstein J. Nanotechnol.* **2018**, 9, 250.
  57. Nasr, M.; Soussan, L.; Viter, R.; Eid, C.; Habchi, R.; Miele, P.; Bechelany, M. High Photodegradation and Antibacterial Activity of BN-Ag/TiO<sub>2</sub> Composite Nanofibers Under Visible Light. *New J. Chem.* **2018**, 42, 1250-1259.
  58. Gottenbos, B.; Grijpma, D. W.; van der Mei, H. C.; Feijen, J.; Busscher, H. J. Antimicrobial Effects of Positively Charged Surfaces on Adhering Gram-Positive and Gram-Negative Bacteria. *J. Antimicrob. Chemother.* **2001**, 48, 7-13.
  59. Fang, W.; Han, C.; Zhang, H.; Wei, W.; Liu, R.; Shen, Y. Preparation of Amino-Functionalized Magnetic Nanoparticles for Enhancement of Bacterial Capture Efficiency. *RSC Adv*. **2016**, 6, 67875-67882.
  60. Fedtke, I.; Götz, F.; Peschel, A. Bacterial Evasion of Innate Host Defenses-The *Staphylococcus aureus* Lesson. *Int. J. Med. Microbiol.* **2004**, 294, 189-194.
  61. Tang, Y.; Xiao, C.; Ding, J.; Hu, K.; Zheng, K.; Tian, X. Synergetic Enhancement of Thermal Conductivity in the Silica-Coated Boron Nitride (SiO<sub>2</sub>@BN)/Polymethyl Methacrylate (PMMA) Composites. *Colloid Polym. Sci.* **2020**, 298, 385-393.
  62. Liu, B.; Qi, W.; Tian, L.; Li, Z.; Miao, G.; An, W.; Liu, D.; Lin, J.; Zhang, X.; Wu, W. *In Vivo* Biodistribution and Toxicity of Highly Soluble PEG-Coated Boron Nitride in Mice. *Nanoscale Res. Lett.* **2015**, 10, 478.
  63. Mukheem, A.; Muthoosamy, K.; Manickam, S.; Sudesh, K.; Shahabuddin, S.; Saidur, R.; Akbar, N.; Sridewi, N. Fabrication and Characterization of an Electrospun PHA/Graphene Silver Nanocomposite Scaffold for Antibacterial Applications. *Materials (Basel)*. **2018**, 11, 1673.
  64. You, C.; Han, C.; Wang, X.; Zheng, Y.; Li, Q.; Hu, X.; Sun, H. The Progress of Silver Nanoparticles in the Antibacterial Mechanism, Clinical Application and Cytotoxicity. *Mol. Biol. Rep.* **2012**, 39, 9193-9201.
  65. Ferdous, Z.; Nemmar, A. Health Impact of Silver Nanoparticles: A Review of the Biodistribution and Toxicity Following Various Routes of Exposure. *Int. J. Mol. Sci.* **2020**, 21, 2375.
  66. Leino, V.; Airaksinen, R.; Viluksela, M.; Vähäkangas, K. Toxicity of Colloidal Silver Products and Their Marketing Claims in Finland. *Toxicol. Rep.* **2020**, 8, 106-113.
  67. Białek, M.; Czauderna, M.; Krajewska, K.; Przybylski, W. Selected Physiological Effects of Boron Compounds for Animals and Humans. A review. *J. Anim. Feed Sci.* **2019**, 28, 307-320.

**Publisher's Note** The Polymer Society of Korea remains neutral with regard to jurisdictional claims in published articles and institutional affiliations.